CSIRO PUBLISHING

RESEARCH PAPER
https://doi.org/10.1071/WF25135

International Journal of Wildland Fire
International Association of Wildland Fire

Flame spread along horizontal fuel particles in the wind

Mark A. Finney[A,*], Ethan J. Levin[A], Nathan P. Kahla[A], Ian J. Grob[A] and Isaac C. Grenfell[A]

For full list of author affiliations and declarations see end of paper

***Correspondence to:**
Mark A. Finney
USDA Forest Service, Missoula Fire Sciences Laboratory, 5775 Highway 10 West, Missoula, MT 59808, USA
Email: mark.finney@usda.gov

Received: 28 May 2025
Accepted: 11 December 2025
Published: 5 February 2026

Cite this: Finney MA *et al.* (2026) Flame spread along horizontal fuel particles in the wind. *International Journal of Wildland Fire* **35**, WF25135. doi:10.1071/WF25135

ABSTRACT

Background. Horizontally continuous fuel types such as pine litter can sustain flame spread along individual fuel particles, but little is known about how wind affects flame behavior at this fine scale. **Aims.** We conducted experiments to examine flame spread rates along thin horizontal fuel particles (cardboard and pine needles) where wind speed and particle orientation relative to wind direction were varied. **Methods.** The wind speed was controlled by mounting a fuel sample on a rotating disk turning at a specified rate. **Key results.** Video measurements showed that flame spread rates on fuel samples varied with fuel orientation angle and wind speed according to the polar equation for an ellipse. The heat transfer mechanism for a wind-blown laminar flame is gas-phase conduction at millimeter scales, the same as with flame spread in opposed flow conditions on other thin cellulosic fuels. **Conclusions.** Flame spread rate was directly related to the angle within the flame volume intercepted by the fuel particle. **Implications.** Despite the short range of gas conduction heating, the elliptical shape implied by the data offers a small-scale physical example of the common assumption that 2D wildland fire shapes can be approximated as ellipses.

Keywords: ellipse, fire shape, flame shape, flame spread, fuel bed, fuel particles, horizontal fuel, pine needles, spread rate.

Introduction

Horizontally continuous litter fuels enable wildfire spread both along individual fuel particles and across the aggregated fuel bed. Pine litter, a horizontally continuous fuel type, has long been used for fire behavior experiments (e.g. Curry and Fons 1938; Nelson and Adkins 1986; Fernandes *et al.* 2009; Campbell-Lochrie *et al.* 2023). Most studies, however, have focused on fire behavior at the fuel bed scale without investigating the contribution of individual particles to the emergent spread patterns (Lyons and Weber 1993). This distinction between particle- and bed-scale behavior is particularly relevant in opposed flow configurations – such as backing fires and spread without wind or slope – where outward flame advection is minimal. In opposed flow cases, flames are deflected away from the spread direction (Beaufait 1965; Mendes-Lopes *et al.* 2003; Viegas 2004*a*; Rossa *et al.* 2015), reducing convective heating and the radiation view factor. Under strong wind conditions, heat transfer may become insufficient to ignite discrete fuel particles separated by air gaps, but continuous litter beds with interlaced fuel elements can still support spread along individual fuel particles by means of gas-phase conduction (Weber and de Mestre 1990; Korobeinichev *et al.* 2018).

Gas-phase conduction is a well-documented mechanism in opposed flow flame spread on thin solid cellulosic fuel particles such as paper and pine needles (Fernandez-Pello and Hirano 1983; Weber and de Mestre 1990). In this process, gases in the attached laminar flame directly contact the fuel surface millimeters ahead of the pyrolyzing edge. Experiments and modeling confirm that flame gas contact is responsible for driving flame spread along *Pinus sylvestris* needles (Korobeinichev *et al.* 2018, 2022), paper strips (Hirano *et al.* 1974*a*, 1974*b*) and wooden dowels (Lai *et al.* 2020). External radiant flux (Hirano and Tazawa 1978; Fernandez-Pello and Hirano 1983) enhances this spread, suggesting that reduced radiation view factor may explain slower downhill flame spread rates on pine needles, paper strips (Hirano *et al.* 1974*a*; Hirano and Tazawa 1978; Weber and de Mestre 1990) and entire fuel beds (Van Wagner 1988; Dupuy 1995; Mendes-Lopes *et al.* 2003; Boboulos and Purvis 2009; Sullivan *et al.* 2014). In contrast, some studies report that backing fires change little or increase slightly with opposing wind (Viegas 2004*b*; Rossa *et al.* 2015; Selvaraj *et al.* 2024).

Weber (1990*a*) and Lyons and Weber (1993) noted that spread rates along single pine needles and across fuel beds are similar in no-wind conditions, but no published work has thoroughly examined flame spread along isolated horizontal fuel elements under wind. The present study addresses this gap by experimentally investigating wind-influenced flame spread along thin cardboard particles – precisely controlled analogs to natural elements such as dead conifer needles, thatched grasses and matted dead vegetation.

Methods

We conducted experiments to examine flame spread along narrow cardboard fuel elements in controlled airflow (Fig. 1). Experience with a small wind tunnel (McAllister *et al.* 2012) demonstrated the difficulty of controlling airspeeds below approximately 0.5 m s^{-1}, required for sustaining opposed flow flame spread on discrete fuel particles. The problem was thus approached by regulating movement of the fuel rather than the air.

Our apparatus consisted of a 3.175 mm thick aluminium disk of 0.406 m radius (r) mounted on a rotary 'welding positioner' operated by an electric motor with continuously variable rotation speed. Rotation speed was controlled by a manual dial that was calibrated to produce known airspeeds or tangential velocity (v) up to a maximum of 0.615 m s^{-1} at the outermost radius (Table 1). A wire stand, 0.1 m tall, was attached vertically to the disk at maximum radius to support a single horizontal cardboard fuel sample. The wire was threaded to permit the fuel sample to be screwed on through a hole in the base (Fig. 2). The entire apparatus was installed on a table in a closed room to limit extraneous air circulations.

Boundary layer effects from the spinning disk were negligible: the laminar layer generated on the surface of a smooth disk in open air is only a few millimeters thick (Littell and Eaton 1994), far below the sample height of 0.1 m. Calculated centripetal acceleration (v^2/r) never exceeded 0.94 m s^{-2} – an order of magnitude lower than buoyant acceleration for flames – indicating that buoyancy and tangential airflow dominated flame behavior (Table 1).

Fuel particles of various widths were manufactured with a CO_2 laser cutter from commercial 'chipboard' with

Table 1. Characteristics of the spinning disk at 0.406 m radius for flame spread experiments.

Rotation frequency (Hz)	Tangential air velocity (m s^{-1})
0.045	0.116
0.091	0.233
0.139	0.355
0.189	0.483
0.241	0.615

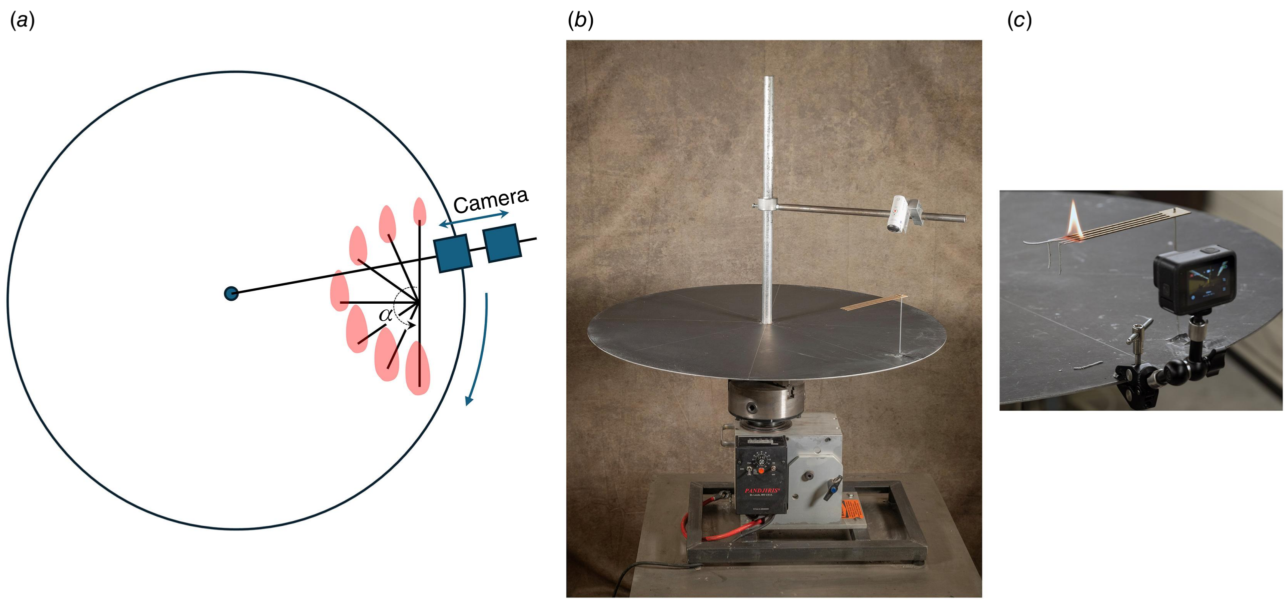

Fig. 1. (*a*) Sketch of spinning disk apparatus showing fuel sample with attached flames, wind direction relative to flame spread direction (α) and camera locations; (*b*) photograph of disk, fuel sample and camera mounted for recording spread rate; and (*c*) camera mounted to record flame angle.

material density of 600 kg m^{-3} (Fig. 2, Table 2). Several designs of cardboard particles were tested, including individual tines and groups of four tines 1.65 and 3.175 mm wide. As wind speed increased, we found that it was difficult to sustain flame spread along individual tines in the backing directions and, therefore, created fuel samples with quadruple tines with separation equal to their widths (Table 2).

Fig. 2. Photograph of cardboard fuel elements used in experiments: (*a*) quadruple 1.578 mm wide, (*b*) quadruple 3.175 mm wide, (*c*) single 3.155 mm wide, and (*d*) single 1.578 mm wide.

This configuration was somewhat arbitrary but based on the morphology of pine foliage, which bears fascicles of two to five needles depending on species. To compare with Weber and de Mestre's (1990) data, individual ponderosa pine needles (density 510 kg m^{-3}) were also tested. All fuel samples were oven-dried at 100°C for 24 h to reduce moisture contents uniformly to 3%.

Quadruple fuel samples were burned at various rotation rates to generate air flow speeds of 0.116, 0.233, 0.355, 0.483 and 0.615 m s^{-1} at 0.406 m disk radius. To control spread direction relative to the wind, tests were conducted with fuel particles oriented at 0°, 30°, 60°, 90°, 120°, 150° and 180° relative to the rotation direction (Fig. 1). The ends of the fuel samples were ignited with a butane lighter while at a standstill until a coherent flame zone developed. The weld positioner motor was turned on to a preset velocity, which accelerated the disk nearly instantaneously. Spread became steady within a few seconds, and the subsequent rate of spread measurements were each considered to represent a steady state.

Flame spread rate along the fuel samples was measured on video taken from a downward-looking camera recording at 60 frames s^{-1} (fps). The camera was suspended from a radial arm above the disk and was thus stationary with respect to the location of a fuel sample as the disk rotated. Flame spread rates on each fuel sample were calculated from the elapsed arrival times of the visible charred edge at pencil markings every 0.025 m. Spread rates from these intervals were used as independent samples (Gould *et al.* 2017). Flames were allowed to spread the entire length of the sample within view of the camera. No data were recorded if spread did not reach the end of the cardboard tine for a certain angle and wind speed. Failure of sustained spread occurred for backing spread directions and higher wind speeds. Ten tests were performed for each combination of wind speed and fuel orientation. Ten no-wind–no-slope tests for each type of fuel sample were done for comparison.

Wind speed was calculated separately for each measured segment (0.025 m) when particles were oriented at angles of 0°, 30°, 60°, 120°, 150° and 180° relative to the wind direction. This was necessary because flames burning

Table 2. Properties of fuel particle samples and tests conducted.

Material	Particle thickness (mm)	Particle width (mm)	Surface area/ volume (m^2 m^{-3})	Particle number	Particle separation (mm)	Length (mm)	Wind speed (m s^{-1})
Cardboard*	1.397	3.175	2062	1	–	152	0–0.483
Cardboard	1.397	3.175	2062	4	3.175	152	0–0.615
Cardboard	1.397	1.587	2691	1	–	152	0–0.483
Cardboard	1.397	1.587	2691	4	1.650	152	0–0.615
Ponderosa pine needles*	~0.7	~0.7	5770	1	–	100	0–0.116

*Cardboard has a material density of 600 kg m^{-3} and ponderosa pine needles were assumed to be 510 kg m^{-3} (Brown 1970). Cardboard has a rectangular cross-section, and needles are approximately triangular.

along the straight particles are advancing outward toward the edge of the disk and thus burning under increasing radius and, thus, increasing wind speed. We found that at 90° from the wind direction, flame spread rate along the element was constant, independently of changing wind speeds for the ranges tested.

We examined flame angle, measured from vertical, as it varied with wind speed and spread direction using a video camera mounted at a radius outside the disk and leveled along the plane of the fuel sample (Fig. 1). For this test, we used single and quadruple tines 3.175 mm wide. Flames spreading along the fuel samples were imaged at 60 fps against a black background. Rotation speeds were varied for the entire range described above for fuel orientations of 0° and 180° for heading and backing spread, respectively. A series of 30 sequential frames (0.5 s) was selected to capture flames in profile as the combustion interface of the flame zone moved in radial alignment between the axle and the camera. The flame angle (measured from vertical) in each image was determined from the slant of the long edge of a parallelogram bounding the flame. The parallelogram was fitted to each of 30 images for a given wind speed test and the median and maximum absolute deviation (MAD) calculated for each test.

For each tine configuration, the interval spread rate data from all replicates were pooled and analyzed by non-linear regression to examine the effects of wind speed and fuel orientation angle. Following Weber and de Mestre (1990), we tested the applicability of the polar equation for an ellipse to describe measurements of spread rate R (m min^{-1}):

$$R = \frac{a}{1 - b\sin\theta} \tag{1}$$

where a is the semi-latus rectum, b is the eccentricity and θ (°) the fuel particle tilt angle from horizontal. For our purposes, we modified this formulation to incorporate wind speed U (m s^{-1}) and used the cosine of flame spread direction relative to the angle the wind is coming from (α):

$$R = \frac{a}{1 + bU\cos\alpha} \tag{2}$$

The polar equation implies flames spread outward from the rear focus of an ellipse and comports with observations that spread rate perpendicular to the wind direction was constant. Spread rates defined normal to an elliptical fire front would not be wind-neutral at an angle of 90° (Catchpole *et al.* 1982).

Results

We found that flame spread rates along the cardboard tines were well described by Eqn 2 (Table 3, Fig. 3) where the eccentricity b of the elliptical function is linearly related to wind speed. The fitted coefficient a represents the uniform spread rate without wind and at 90° for all wind speeds. Variation in measured spread rates increased toward the

Table 3. Measurements from flame spread tests along cardboard tines and pine needles (means and standard deviation, s.d.) along with fitted model parameters a and b (and standard errors, s.e.) for Eqn 2.

Material	Tine width (mm)	Number of tines	R (s.d.) no wind (m min^{-1})	R (s.d.) at 90° (m min^{-1})	a (s.e.) (m min^{-1})	b (s.e.) (m min^{-1})	Wind speed and α spread limit angle (m s^{-1})
Cardboard	3.175	1	0.0696 (0.005)	0.0739 (0.0076)	0.0844 (0.001)	1.3517 (0.0117)	0.483, ≤120° 0.355, ≤120° 0.173, ≤180°
Cardboard	3.175	4	0.0908 (0.0075)	0.0870 (0.0072)	0.0925 (0.0008)	1.1442 (0.0058)	0.615, ≤120° 0.483, ≤150° 0.355, ≤180°
Cardboard	1.650	1	0.1076 (0.0126)	0.1011 (0.011)	0.1112 (0.0014)	1.518 (0.0163)	0.418, ≤120° 0.233, ≤120° 0.116, ≤180°
Cardboard	1.650	4	0.1089 (0.0143)	0.091 (0.011)	0.1085 (0.0015)	1.169 (0.0081)	0.615, ≤90° 0.483, ≤90° 0.355, ≤180°
Ponderosa pine needle	~0.7	1	0.1341 (0.0307)	0.151 (0.0433)	0.1373 (0.0025)	1.538 (0.1817)	

Sustained flame spread was not observed beyond the angle limit listed for a given wind speed but was for all angles (0°–180°) at lower wind speeds.

heading direction (Fig. 3*a*) and the fire length/breadth ratio increased as an exponential-type function of wind (Fig. 4).

A two-tailed *t*-test for each tine configuration indicated that spread rates at 90° from the wind direction were not statistically different than without wind (Table 3, Fig. 3). Spread rates were faster along thinner tines but eccentricity was comparable. Flame spread rate along single cardboard tines was similar to quadruple configurations but much faster on single ponderosa pine needles than the cardboard (Table 3). The standard deviation for spread rate on pine needles was approximately triple the measured values from both single and quadruple cardboard tines perhaps owing to needle curvature or unknown variations in needle composition.

Flame spread thresholds were observed to depend on the tine configuration (Table 3), with flame spread sustained on quadruple tines at greater wind speeds at greater angles than on single tines.

Flame spread rate was strongly correlated with flame tilt angle (Figs 5 and 6, Table 4). This finding is in accord with experiments of Weber (1990*a*) who modeled spread rate as a function of the tilt angle θ of ponderosa pine needles relative to a vertical flame. To compare with Weber's (1990*a*) results, we substituted our fitted values for cardboard (3.175 mm wide) from Table 3 for Weber's a parameter but used his experimentally determined value of eccentricity (b = 0.8) in Eqn 1. The consistency in spread rate trends between our wind data and Weber's (1990*a*) flame tilt model (Fig. 6) suggested that flame spread by gas-phase conduction is likely a product of the length of fuel intercepted by the flame volume. Tilting of flame or fuel produces a similar fuel heating length and thus flame spread rate. The exact profile of the flame volume as it intercepts horizontal fuel particles is not interpretable from our data (i.e. Fig. 4) but Eqn 2 implies fires would be elliptical under these idealized conditions.

Discussion

No previous studies of two-dimensional fire growth have directly linked the effects of wind on fuel particle spread with resulting fire shape. Data from this experiment suggest that an elliptical shape emerges when laminar flames are allowed to spread in an idealized growing fire. The shape of

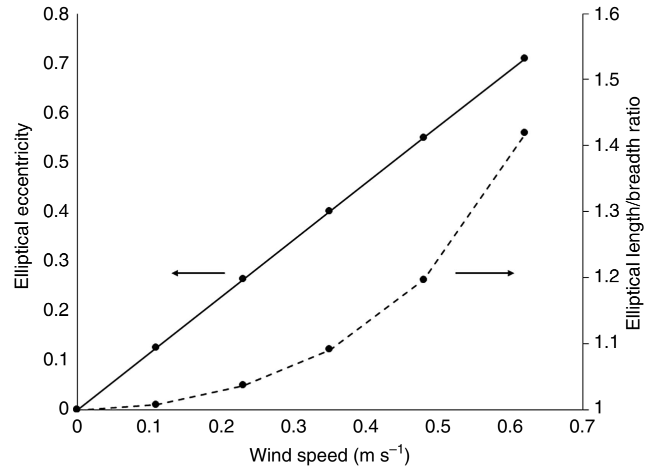

Fig. 4. Experimental results from quadruple 3.175 mm fuel samples showing eccentricity and length/breadth ratio of ellipses from Eqn 2.

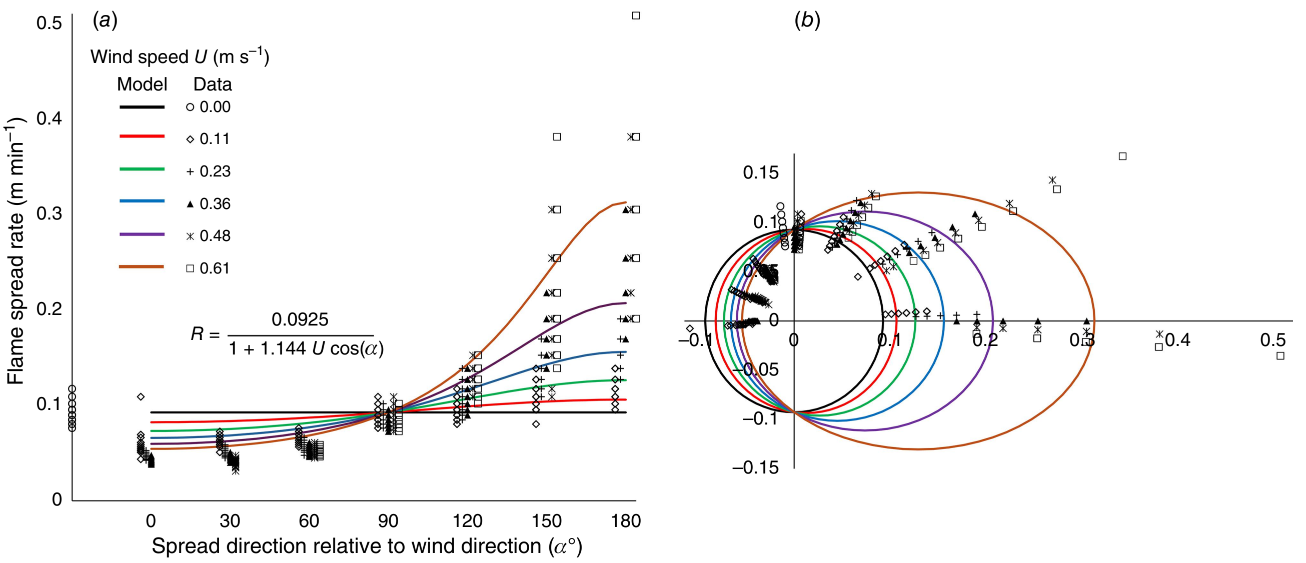

Fig. 3. Experimental results from quadruple 3.175 mm fuel samples showing: (*a*) flame spread data and polar ellipse model (Eqn 2, Table 3) for each windspeed and wind direction (α); and (*b*) data and elliptical shapes of fires from the fitted model in Cartesian coordinates. Note that data are displayed offset from actual α to distinguish different wind speeds.

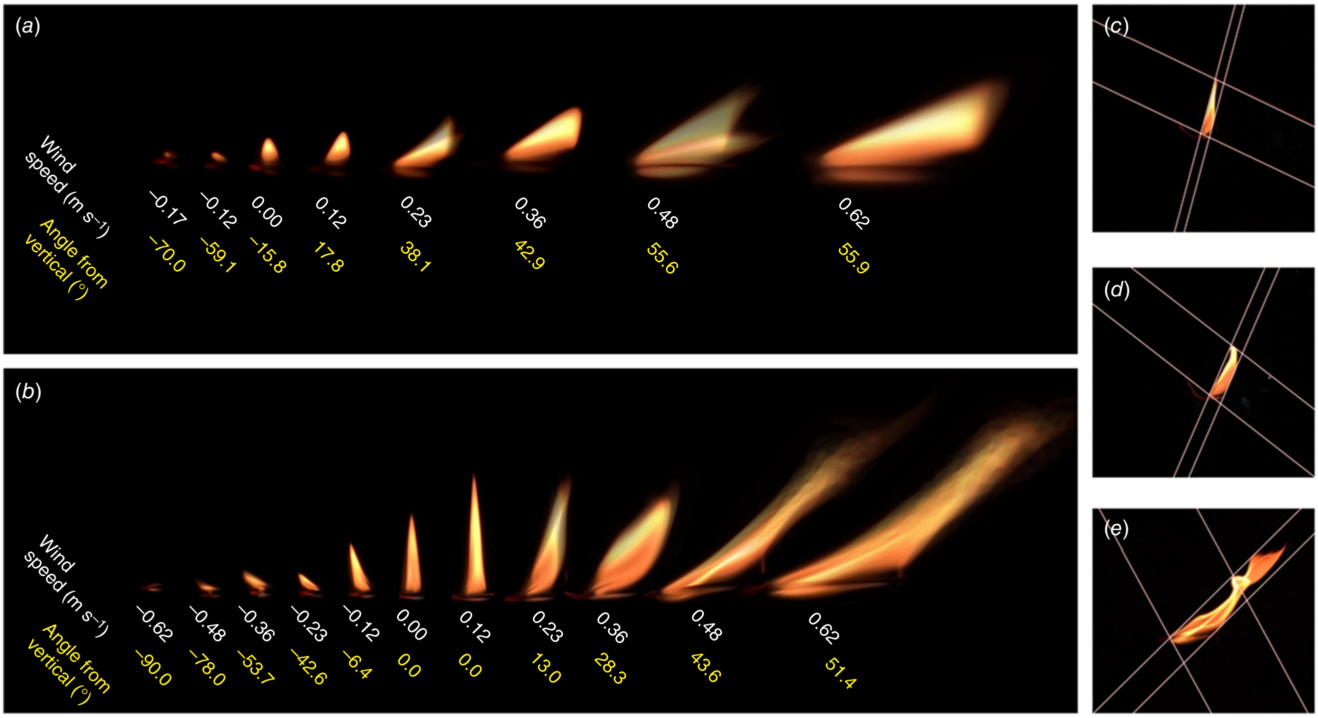

Fig. 5. Composite of photographs showing flame angle from vertical as a function of wind speeds for: (*a*) single 3.175 mm cardboard fuel samples, and (*b*) quadruple 3.175 mm cardboard fuel samples, and examples of parallelogram analysis used for determining flame angle from vertical for different wind speeds (*c*) 0.23 m s^{-1}, (*d*) 0.36 m s^{-1}, and (*e*) 0.62 m s^{-1} (aligned with spread direction).

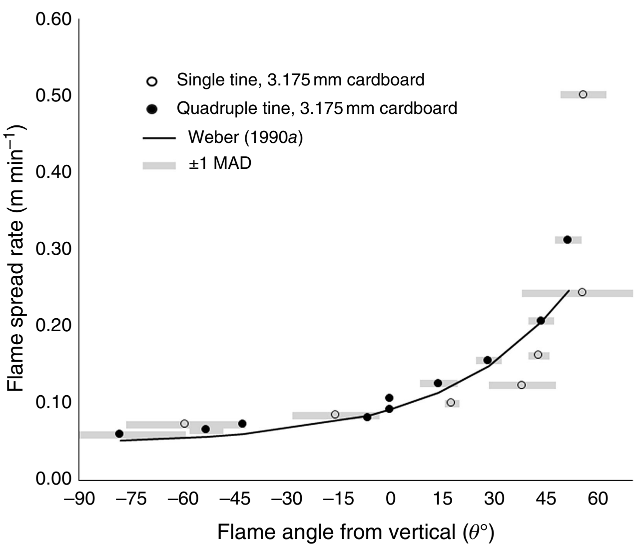

Fig. 6. Comparison of mean flame angle and spread rate from tests using 3.175 mm cardboard fuel samples (single and quadruple tines) with Eqn 1 from Weber (1990*a*) for spread along fuel particles tilted relative to a vertical flame. Wind-blown flame angle from the vertical was determined as the median of 30 sequential images for each wind speed as the slant of the long edge of a parallelogram bounding the flame. MAD is the maximum absolution deviation from the median flame angle.

a growing fire in a fuel bed, whether in the laboratory or in the field, is affected by interactions among portions of the flame front or influences of environmental heterogeneities. For example, flames in laboratory-scale spreading fires are often large relative to the dimensions of the burning area (Viegas 2004*a*; Viegas *et al.* 2024), creating interference among induced airflows. These airflows together with the heated interior region influence fire growth, as indicated by the inward tilt of flames.

Point-source ignitions in litter fuel beds have been widely used to examine fire shapes, with studies reporting only one axis of symmetry, such as double ellipses or ovoids (Curry and Fons 1938; Peet 1967; Anderson 1983; Viegas *et al.* 2024). On sloping surfaces, pointed shapes can also arise when vorticity propagates forward along the flame front (Dupuy *et al.* 2011; Viegas *et al.* 2024). Field-scale experiments offer less control over wind and fuel variations but may reduce flame interactions as fire fronts broaden beyond laboratory scales. In both laboratory and field experiments, point ignitions accelerate and evolve in shape over time (McAlpine and Wakimoto 1991; Cheney and Gould 1995, 1997; Gould and Sullivan, 2022), which means that fire spread rate and its two-dimensional variation would be transient during this phase of fire growth.

The strong fit of the polar ellipse (Eqn 2) to our data implies that flames were spreading outward from the rear

Table 4. Median flame tilt angle from vertical and modeled flame spread rates (Eqn 2, Table 3) on single tines and quadruple tine fuel samples 3.175 mm wide for the range of wind speeds.

Wind speed (m s^{-1})	Median flame angle one tine (θ°)	MAD one tine[A] (θ°)	Flame spread rate, one tine (m min^{-1})	Median flame angle four tines (θ°)	MAD four tines[A] (θ°)	Flame spread rate, four tines (m min^{-1})
-0.62				-90.0	–	0.054
-0.48				-78.01	17.773	0.060
-0.36				-53.07	3.809	0.066
-0.23	-70.0	–	0.064	-42.58	0.760	0.073
-0.12	-59.10	16.071	0.086	-6.43	0.564	0.082
0.00	-15.76	11.466	0.100	0.00	0.000	0.093
0.12	17.76	1.014	0.119	0.00	0.000	0.107
0.23	38.06	8.627	0.147	13.97	4.421	0.126
0.36	42.92	2.088	0.194	28.32	2.649	0.156
0.48	55.58	16.832	0.295	43.61	2.674	0.207
0.62	55.88	5.577	0.633	51.39	2.861	0.313

Maximum absolute deviation (MAD) is shown for flame angle at each wind speed.
[A]Single image was used at wind speeds where flames would not sustain spread (no MAD).

focus. The rear focus is the assumed ignition point for elliptical fire shapes (Alexander 1985) and the basis for Huygens' principle (Anderson *et al.* 1982; Richards 1990) and minimum travel time models (Finney 2002). Our isolated fuel samples preserve the independence of spread for all points on a fire's edge assumed by these methods. However, the fire expansion rate from the rear focus is not the same as the normal *fire spread rate* defined by Catchpole *et al.* (1982), which extends outward perpendicular to the flame front. Both normal and focal spread rates have been used for modeling 2D fire growth (Roberts 1993). But clearly the normal angle formulation would not be appropriate to describe our data because spread at 90° was wind-independent. Experiments by André *et al.* (2013) examined spread from line segments oriented at different angles on a sloping bed but no experiments have yet tested whether spread of a linear segment of flame front at different angles to the wind would vary as an elliptical function like spread on individual particles. Such experiments would be invaluable to understand how local-scale processes (heat transfer, ignition) interact with fire-scale dynamics in producing fire shapes.

Our data suggested that eccentricity of the elliptical fire shape (Eqn 2) would increase linearly with wind speed (Fig. 4). This relationship adequately describes our data but cannot be extrapolated to higher winds indefinitely because eccentricity is bounded at a value of one. More data would be required to suggest another functional form. Still, the linear trend is comparable with the increase in eccentricity at low wind speeds observed in empirical length–width formulae for 2D fire shapes (Anderson 1983; Alexander 1985; Andrews 2018). Fire shape models from Anderson (1983) and Andrews (2018) use a 'mid-flame' wind whereas Alexander (1985) uses a 10 m wind. Our maximum wind speed of 0.615 m s^{-1} is local to the surface of each fuel sample and far slower than the range of mid-flame or 10 m winds. Our wind speeds are more similar to within-bed measurements (Rossa *et al.* 2015), typically <0.5 m s^{-1} for free-stream winds up to 3 m s^{-1} across different fuel packings (Mueller *et al.* 2021).

Backing spread on our isolated fuel samples was highly sensitive to wind speed and suggests that a different characteristic wind velocity could apply to rear-facing spread directions compared with heading and forward-facing spread. As wind speed increased, gas-phase conduction along individual fuel strands was only sustained at angles closer to the wind direction, causing spread to truncate first at the rear and progressively approach the head as winds increased. In backing fires, the wind must pass through unburned fuel before reaching the flame front and is heavily attenuated by the bulk properties of the fuel bed and surface roughness (Rossa *et al.* 2015; Mueller *et al.* 2021). By contrast, winds impinging on heading fires convectively heat fuel particles by advecting flames forward and downward from the combustion interface (Finney *et al.* 2015; Cohen and Finney 2023*b*). Winds impinging on the head fire are modified by the flaming region, the burned fuel profile and heated ground behind the flame zone. The idea of a 'mid-flame' wind (Rothermel 1972) would thus mean something different in each case if the wind affecting the location of heat transfer to the fuel material is considered.

An intriguing result of this experiment was the insensitivity of particle flame spread rate to wind speed at $\alpha = 90°$. Across all wind speeds, the spread rate at 90° was statistically indistinguishable from the no-wind–no-slope spread rate

(Table 3). Few studies have measured spread in lateral directions and they often refer generally to flanking spread simply as the widest part of an ellipse (Van Wagner 1969). But in pine needle beds, Anderson (1983) reported data from point-source fires showing spread at 90° slowed with increasing wind speed. Additional study is needed to determine whether or how such contradictions may be related to the difference between flame spread on single particles versus fire growth across fuel beds.

Laminar flame spread on individual fuel elements is very different than spread of turbulent flames in large wildfires. Still, our experiments provide a physical example of elliptical spread that may scale up where flame contact is limiting heat transfer. The dependence of spread rate on flame angle (Fig. 6) suggests that laminar flame spread is driven by gas conduction where fuel particles intersect the flame volume. Flames leaning forward with the wind intersect longer sections of fuel materials than flames leaning against it (Fig. 5), just as with tilting the particle relative to a vertical flame (Weber and de Mestre 1990). When the fuel orientation angle varies in two dimensions, the intersection distance for a given flame tilt (or wind speed in this case) reflects the heating length within the flame volume like a 'conic section'. Although our data cannot confirm this directly (because flame volume is not constant and grows with tilt and spread rate (Weber and de Mestre 1990)), the analogy does support a long-suspected geometric basis for flame spread (Weber 1990*b*). Large fires with turbulent flames demonstrate similar reliance on flame contact for heating fuel particles (Finney *et al.* 2015; Cohen and Finney 2023*a*, 2023*b*). Fire spread and convective heating are enhanced by flame advection forward of the combustion interface in windward and uphill directions (Dupuy *et al.* 2011; Finney *et al.* 2022). Even without slope-induced changes in flame angle for line fires (Wu *et al.* 2000), inclination of the fuel surface produces the equivalent tilt of the fuel bed relative to the flame like a non-normal section through a volume of revolution (Weber 1990*a*, 1990*b*; Lyons and Weber 1993; Finney *et al.* 2010; Yedinak *et al.* 2010). Wind tilts the flame away from backing or flanking spread directions, providing minimal intermittent flame contact, and requires other processes such as gas-phase conduction if spread is to continue. This study examines one such process, but basic questions remain as to how fire behavior at fuel bed scales emerges from flame spread at fuel particle scales (Weber 1990*b*; Lyons and Weber 1993).

More research is required to understand if, or how, particle-scale results extend to different full-scale wildfire behaviors. Intraparticle flame spread and gas-phase conduction may be of limited relevance in some heading fires when radiant and convective heating are sufficient to ignite fuel particles far beyond length-scales of individual fuel particles. Fine-scale gas conduction is more likely to influence fire behavior in continuous fuels under opposed flow or backing configurations. Our particle spread rates appear slightly slower than typical values for backing and no-wind fires (depending on fuel bed properties), but the decline with increasing wind is similar to laboratory studies that report slight decreases in backing spread rate (Anderson 1983; Mendes-Lopes *et al.* 2003; Boboulos and Purvis 2009) or little wind effect (Beaufait 1965; McAlpine and Wakimoto 1991; Viegas 2004*a*; Fernandes *et al.* 2009; Rossa *et al.* 2015; Selvaraj *et al.* 2024). Downslope spread on particles and in concurrent flow has been investigated more extensively (Hirano *et al.* 1974*a*; Hirano and Tazawa 1978; Weber 1990*a*; Weber and de Mestre 1990) and particle trends are comparable with fuel bed studies that show decreasing spread rates with slope angle up to ∼20°–30° (Van Wagner 1988; Dupuy 1995; Mendes-Lopes *et al.* 2003; Boboulos and Purvis 2009; Sullivan *et al.* 2014). This is likely to occur because upslope flame tilt reduces heat transfer downhill to unburned fuel. Even if larger-scale effects such as radiation, convection and induced airflows are considered, extending particle-scale behaviors to fuel beds will require statistical methods to account for variability in three-dimensional particle orientation, fuel particle intersections and local airflow.

Conclusions

Flame spread experiments on isolated fuel samples were conducted over a range of windspeeds up to 0.615 m s^{-1} and orientation angles 0°–180° from the wind direction. We found that flame spread rate was a polar elliptical function of fuel orientation angle with eccentricity increasing with wind speed. Spread rates normal to the wind direction were independent of windspeed and defined the semi-latus rectum of the elliptical fire shape. The spread rate was related to wind-tilted flame angles much like when fuel particles are tilted relative to a vertical flame. These experiments confirm findings from no-wind conditions that flame spread on individual fuel elements is explained by gas-phase conduction.

References

Alexander ME (1985) Estimating the length-to-breadth ratio of elliptical forest fire patterns. In 'Proceedings of the 8th Conference Fire and Forest Meteorology'. pp. 85–104. (Society of American Foresters: Detroit, MI, USA)

Anderson HE (1983) Predicting wind-driven wildland fire size and shape. Research Paper INT-305. (USDA Forest Service, Intermountain Forest and Range Experiment Station)

Anderson DH, Catchpole EA, De Mestre NJ, Parkes T (1982) Modelling the spread of grass fires. *The ANZIAM Journal* **23**(4), 451–466. doi:10.1017/S0334270000000394

André JC, Gonçalves JC, Vaz GC, Viegas DX (2013) Angular variation of fire rate of spread. *International Journal of Wildland Fire* **22**(7), 970–979. doi:10.1071/WF12028

Andrews PL (2018) The Rothermel surface fire spread model and associated developments: a comprehensive explanation. General Technical Report. RMRS-GTR-371. (USDA Forest Service, Rocky Mountain Research Station)

Beaufait WR (1965) Characteristics of backfires and headfires in a pine needle fuel bed. Research Note INT-39. (USDA Forest Service, Intermountain Forest and Range Experiment Station)

Boboulos M, Purvis MR (2009) Wind and slope effects on ROS during the fire propagation in east-Mediterranean pine forest litter. *Fire Safety Journal* **44**, 764–769. doi:10.1016/j.firesaf.2009.03.006

Brown JK (1970) Physical fuel properties of Ponderosa pine forest floors and cheatgrasses. Research Paper INT-74. (USDA Forest Service, Intermountain Forest and Range Experiment Station)

Campbell-Lochrie Z, Walker-Ravena C, Gallagher M, Skowronski N, Mueller EV, Hadden RM (2023) Effects of fuel bed structure on heat transfer mechanisms within and above porous fuel beds in quiescent flame spread scenarios. *International Journal of Wildland Fire* **32**(6), 913–926. doi:10.1071/WF22129

Catchpole EA, de Mestre NJ, Gill AM (1982) Intensity of fire at its perimeter. *Australian Forest Research* **12**, 47–54.

Cheney NP, Gould JS (1995) Fire growth in grassland fuels. *International Journal of Wildland Fire* **5**(4), 237–247. doi:10.1071/WF9950237

Cheney NP, Gould JS (1997) Letter to the editor. Fire growth and acceleration. *International Journal of Wildland Fire* **7**(1), 1–5. doi:10.1071/WF9970001

Cohen JD, Finney MA (2023*a*) Fuel particle heat transfer; part 1: Convective cooling of irradiated fuel particles. *Combustion Science and Technology* **195**(13), 3095–3121. doi:10.1080/00102202.2021.2019231

Cohen JD, Finney MA (2023*b*) Fuel particle heat transfer; part 2: Radiation and convection during spreading laboratory fires. *Combustion Science and Technology* **195**(13), 3122–3147. doi:10.1080/00102202.2021.2019232

Curry JR, Fons WL (1938) Rate of spread of surface fires in the ponderosa pine type of California. *Journal of Agricultural Research* **57**(4), 239–267.

Dupuy JL (1995) Slope and fuel load effects on fire behavior: laboratory experiments in pine needles fuel beds. *International Journal of Wildland Fire* **5**(3), 153–164. doi:10.1071/WF9950153

Dupuy JL, Maréchal J, Portier D, Valette JC (2011) The effects of slope and fuel bed width on laboratory fire behaviour. *International Journal of Wildland Fire* **20**(2), 272–288. doi:10.1071/WF09075

Fernandes PM, Botelho HS, Rego FC, Loureiro C (2009) Empirical modelling of surface fire behaviour in maritime pine stands. *International Journal of Wildland Fire* **18**(6), 698–710. doi:10.1071/WF08023

Fernandez-Pello A, Hirano T (1983) Controlling mechanisms of flame spread. *Combustion Science and Technology* **32**(1-4), 1–31. doi:10.1080/00102208308923650

Finney MA (2002) Fire growth using minimum travel time methods. *Canadian Journal of Forest Research* **32**(8), 1420–1424. doi:10.1139/x02-068

Finney MA, Cohen JD, Grenfell IC, Yedinak KM (2010) An examination of fire spread thresholds in discontinuous fuel beds. *International Journal of Wildland Fire* **19**(2), 163–170. doi:10.1071/WF07177

Finney MA, Cohen JD, Forthofer JM, McAllister SS, Gollner MJ, Gorham DJ, Saito K, Akafuah NK, Adam BA, English JD (2015) Role of buoyant flame dynamics in wildfire spread. *Proceedings of the National Academy of Sciences* **112**(32), 9833–9838. doi:10.1073/pnas.1504498112

Finney MA, Grumstrup TP, Grenfell IC (2022) Flame characteristics adjacent to a stationary line fire. *Combustion Science and Technology* **194**(11), 2212–2232. doi:10.1080/00102202.2020.1863952

Gould JS, Sullivan AL (2022) Initial growth of fires in eucalypt litter, from ignition to steady-state rate of spread: laboratory studies. *International Journal of Wildland Fire* **31**(2), 163–175. doi:10.1071/WF21094

Gould JS, Sullivan AL, Hurley R, Koul V (2017) Comparison of three methods to quantify the fire spread rate in laboratory experiments. *International Journal of Wildland Fire* **26**(10), 877–883. doi:10.1071/WF17038

Hirano T, Tazawa K (1978) A further study on effects of external thermal radiation on flame spread over paper. *Combustion and Flame* **32**, 95–105. doi:10.1016/0010-2180(78)90083-4

Hirano T, Noreikis SE, Waterman TE (1974*a*) Postulations of flame spread mechanisms. *Combustion and Flame* **22**(3), 353–363. doi:10.1016/0010-2180(74)90050-9

Hirano T, Noreikis SE, Waterman TE (1974*b*) Measured velocity and temperature profiles near flames spreading over a thin combustible solid. *Combustion and Flame* **23**(1), 83–96. doi:10.1016/S0010-2180(74)80029-5

Korobeinichev OP, Shmakov AG, Osipova KN, Kumar A, Kambam Meetei N (2018) Experimental study and numerical modeling of downward flame spread along a single pine needle: part 1 (experiments). *Combustion Science and Technology* **190**(1), 64–185. doi:10.1080/00102202.2017.1380001

Korobeinichev OP, Kumaran SM, Shanmugasundaram D, Raghavan V, Trubachev SA, Paletsky AA, Shmakov AG, Glaznev RK, Chernov AA, Tereshchenko AG (2022) Experimental and numerical study of flame spread over bed of pine needles. *Fire Technology* **58**, 1–38. doi:10.1007/s10694-021-01190-2

Lai Y, Wang X, Rockett TBO, Willmott JR, Zhou H, Zhang Y (2020) The effect of preheating on fire propagation on inclined wood by multi-spectrum and schlieren visualisation. *Fire Safety Journal* **118**, 103223. doi:10.1016/j.firesaf.2020.103223

Littell HS, Eaton JK (1994) Turbulence characteristics of the boundary layer on a rotating disk. *Journal of Fluid Mechanics* **266**, 175–207. doi:10.1017/S0022112094000972

Lyons PRA, Weber RO (1993) Geometrical effects on flame spread rate for wildland fine fuels. *Combustion Science and Technology* **89**(1–4), 153–165. doi:10.1080/00102209308924106

McAllister S, Grenfell I, Hadlow A, Jolly WM, Finney M, Cohen J (2012) Piloted ignition of live forest fuels. *Fire Safety Journal* **51**, 133–142. doi:10.1016/j.firesaf.2012.04.001

McAlpine RS, Wakimoto RH (1991) The acceleration of fire from point source to equilibrium spread. *Forest Science* **37**(5), 1314–1337. doi:10.1093/forestscience/37.5.1314

Mendes-Lopes JM, Ventura JM, Amaral JM (2003) Flame characteristics, temperature–time curves, and rate of spread in fires propagating in a bed of *Pinus pinaster* needles. *International Journal of Wildland Fire* **12**(1), 67–84. doi:10.1071/WF02063

Mueller EV, Gallagher MR, Skowronski N, Hadden RM (2021) Approaches to modeling bed drag in pine forest litter for wildland fire applications. *Transport in Porous Media* **138**(3), 637–660. doi:10.1007/s11242-021-01637-8

Nelson RM, Adkins CW (1986) Flame characteristics from wind-driven surface fires. *Canadian Journal of Forest Research* **16**, 1293–1300. doi:10.1139/x86-229

Peet GB (1967) The shape of mild fires in Jarrah forest. *Australian Forestry* **31**(2), 121–127. doi:10.1080/00049158.1967.10675433

Richards GD (1990) An elliptical growth model of forest fire fronts and its numerical solution. *International Journal for Numerical Methods in Engineering* **30**(6), 1163–1179. doi:10.1002/nme.1620300606

Roberts S (1993) A line element algorithm for curve flow problems in the plane. *Journal of the Australian Mathematical Society. Series B. Applied Mathematics* **35**, 244–261. doi:10.1017/S0334270000009152

Rossa CG, Davim DA, Viegas DX (2015) Behaviour of slope and wind backing fires. *International Journal of Wildland Fire* **24**(8), 1085–1097. doi:10.1071/WF14215

Rothermel RC (1972) A mathematical model for predicting fire spread in wildland fuels. Research Paper INT-115. (USDA Forest Service, Intermountain Forest and Range Experiment Station)

Selvaraj MK, Vasudevan R, Korobeinichev O, Trubachev S, Paletsky A, Sagitov A, Chernov A, Shmakov A (2024)) effects of fuel bed slope and wind direction on flame spread characteristics over a bed of *Pinus silvestris* needles. *Combustion Science and Technology* **197**, 5217–5237. doi:10.1080/00102202.2024.2393658

Sullivan AL, Sharples JJ, Matthews S, Plucinski MP (2014) A downslope fire spread correction factor based on landscape-scale fire behaviour. *Environmental Modelling & Software* **62**, 153–163. doi:10.1016/j.envsoft.2014.08.024

Van Wagner CE (1969) A simple fire-growth model. *The Forestry Chronicle* **45**(2), 103–104. doi:10.5558/tfc45103-2

Van Wagner CE (1988) Effect of slope on fires spreading downhill. *Canadian Journal of Forest Research* **18**(6), 820–822. doi:10.1139/x88-125

Viegas DX (2004*a*) On the existence of a steady state regime for slope and wind driven fires. *International Journal of Wildland Fire* **13**(1), 101–117. doi:10.1071/WF03008

Viegas DX (2004*b*) Slope and wind effects on fire propagation. *International Journal of Wildland Fire* **13**(2), 143–156. doi:10.1071/WF03046

Viegas DX, Ribeiro C, Barbosa TF, Rodrigues T, Ribeiro LM (2024) A fireline displacement model to predict fire spread. *Fire* **7**(4), 121. doi:10.3390/fire7040121

Weber RO (1990*a*) The moist strand and the burning bed. *Canadian Journal of Forest Research* **20**(6), 845–848. doi:10.1139/x90-111

Weber RO (1990*b*) A model for fire propagation in arrays. *Mathematical and Computer Modelling* **13**(12), 95–102. doi:10.1016/0895-7177(90)90103-T

Weber RO, de Mestre ND (1990) Flame spread measurements on single ponderosa pine needles: effect of sample orientation and concurrent external flow. *Combustion Science and Technology* **70**(1–3), 17–32. doi:10.1080/00102209008951609

Wu Y, Xing HJ, Atkinson G (2000) Interaction of fire plume with inclined surface. *Fire Safety Journal* **35**(4), 391–403. doi:10.1016/S0379-7112(00)00032-1

Yedinak KM, Cohen JD, Forthofer JM, Finney MA (2010) An examination of flame shape related to convection heat transfer in deep-fuel beds. *International Journal of Wildland Fire* **19**(2), 171–178. doi:10.1071/WF07143

Data availability. Data are available on request from the authors.

Conflicts of interest. The authors declare that they have no conflicts of interest.

Declaration of funding. The study was funded by the US Forest Service, National Fire Decision Support Center.

Acknowledgements. Research was supported by the United States Forest Service, Rocky Mountain Research Station, National Fire Decision Support Center. The authors thank Josh Deering for construction of the apparatus and anonymous referees for their comments and suggestions on the manuscript.

Author affiliation

[A]USDA Forest Service, Missoula Fire Sciences Laboratory, 5775 Highway 10 West, Missoula, MT 59808, USA.